Using the root spread information of pioneer plants to quantify their mitigation potential against shallow landslides and erosion in temperate humid climates

Gonzalez-Ollauri, Alejandro; Mickovski, Slobodan B.

Published in:
Ecological Engineering

DOI:
10.1016/j.ecoleng.2016.06.028

Publication date:
2016

Document Version
Author accepted manuscript

Using the root spread information of pioneer plants to quantify their mitigation potential against shallow landslides and erosion in temperate humid climates

Alejandro Gonzalez-Ollauri[1,2] and Slobodan B. Mickovski[1]
[1]School of Engineering & Built Environment, Glasgow Caledonian University
Glasgow, G4 0BA Scotland, UK
[2]Corresponding author: alejandro.ollauri@gcu.ac.uk

Abstract

The aim of this paper was to quantify the mitigation potential of pioneer herbs against shallow landslides and erosion in temperate humid climates and to identify key plant information to aid species selection for slope stabilisation. The objectives ranged from the study of the climate, soil and root spread of three native perennial herbs growing on a landslide-prone slope in Northeast Scotland to the verification of an upgraded spatially distributed eco-hydrological model in order to test whether root spread information can be provided cost-effectively in temperate humid climates. The retrieved information on root spread was then used to evaluate the slope stabilisation potential of the pioneer herbs in the topmost soil horizons using a limit equilibrium method.

The results indicated that pioneer herbs, although presenting climate-influenced shallow root systems, could noticeably contribute to reducing soil mass loss and landslides. This was largely determined by the plant biomass and allometry, the latter being a potential readily measurable proxy for species selection in slope stabilisation that will need further investigation. Additionally, our observations supported the model predictions remarkably well when site-specific inputs were employed, showing that the proposed model is a suitable and cost-effective tool to provide spatial root spread information for eco-engineering purposes in temperate humid climates.

Key words: herb, root spread, temperate humid climate, allometry, distributed model, shallow landslide.

1. Introduction

Landslides and erosion are a global hazard that lead to dramatic loss of human life, property and soil every year with an occurrence that will likely increase due to the effects of climate and land use change (van Beek et al., 2008; IPCC, 2014) if action is not taken.

The use of plants against shallow landslides and erosion has been shown to be an effective eco-engineering measure (Stokes et al., 2014) mainly provided by the soil-root mechanical reinforcement (Norris et al., 2008). A root-permeated soil makes up a composite material that has enhanced strength (Waldron, 1977), providing a similar effect to the soil like that of steel rods to reinforced concrete (Mickovski et al., 2009). However, to quantify the extent of soil-root reinforcement, information on the root spread in the soil is needed to evaluate the slope stabilisation potential of the plant in the topmost soil horizons.

Despite the relatively recent efforts to quantify root spread at a global scale (e.g. Schenk and Jackson, 2002; Schenk and Jackson, 2005), it still remains unknown for the vast majority of the wild plant species. Indeed, information related to pioneer herbs is severely scarce, as far more attention has been traditionally paid to woody plant species (Stokes et al., 2008) and crops (Böhm, 1979). Pioneer herbs may present a great eco-engineering potential as they are fast-growing, easily spreadable and set the basis for further ecological succession (Odum and Barrett, 1971). However, herb's root systems are expected to be limited to the topmost soil horizons, being more likely effective against rill or gully erosion (e.g. van Beek et al., 2008). Hence, the use of

herbs in eco-engineering slope stabilisation actions needs to be combined with other remediation techniques (e.g. Tardio and Mickovski, 2016).

The root distribution in the soil may be complex and, obtaining related information is expensive and time-consuming. Thus, the development of numerical root distribution models has been the scope of research in the past few decades (e.g. Wu et al., 2005) and based on this research, for most practical eco-engineering applications, a root profile can be portrayed as a simple asymptotic mathematical function (Jackson et al., 1996). Additionally, it has been observed that root spread is chiefly influenced by water availability in the soil (i.e. 'hydrotropism'; Darwin, 1880; Tsutsumi, 2003). This concept permits to link the root development to climate and soil properties (Schenk and Jackson, 2002) and, therefore, to the soil's water balance. In this sense, Laio et al. (2006) developed an analytical eco-hydrological model able to predict realistically the rooting depth at the plant community level for water-limited ecosystems (i.e. arid or dry environments) from readily available soil and climatic predictors. These predictors can be easily parameterised from the soil physicochemical properties (i.e. porosity, texture and organic matter content) and from temperature and rainfall information collected by many weather stations. However, the root spread has rarely been assessed using *in situ* soil and climate-derived information as data from distant meteorological stations and sampling locations are normally interpolated for a given study site (e.g. Preti et al., 2010; Tron et al., 2014). Laio´s et al. model was further extended by Preti et al. (2010) to provide plant species-specific root profile information by the consideration of a universal property to all living organisms, the allometry (West et al., 1997). Plants allocate their biomass above and below the ground, and the proportion in which this is distributed can be assessed by the plant's allometric relationship (Cheng and Niklas, 2007)

depicted by a simple power-law relationship (West et al., 1997). This relationship permits to cost-effectively infer the root biomass from measurements of the aboveground biomass and also potentially determine plant parameters related to soil reinforcement purposes (e.g. Hwang et al., 2015). To the best of our knowledge, the identification of plant indicators able to enhance the effectiveness of plant selection against shallow landslides has been rarely explored (e.g. Cornelini et al., 2008). Additionally, the existing models (Laio et al., 2006; Preti et al., 2010) are, essentially, one-dimensional and cannot be readily applied to temperate humid climates (Tron et al., 2014), which cover a big surface of the Earth (Köppen, 1884).

Climate, soil, and plant cover are spatially highly heterogeneous, which stresses the need of adopting spatial approaches to predict root system features under different environmental and landscape scenarios. However, spatially distributed root spread models are lacking in the literature (e.g. O'Brien et al., 2007; Coelho et al., 2003), although these types of models are very popular in hydrology and catchment science (Neitsch et al., 2011; Doppler et al., 2014). The development of distributed root spread models may be very helpful to assess the spatial effect of vegetation against shallow landslides and erosion or to enhance the predictive capacity of other spatial models aiming to quantify plant-derived processes (e.g. water fluxes, nutrient cycles or sediment dynamics at the catchment scale; SWAT; Neitsch et al., 2011). However, the performance of a given distributed model will rely on the quality of the spatial information used as an input. In this sense, the implementation of machine learning techniques, such as the *random forest* algorithm (RF; Breiman, 2001), for predicting spatially heterogeneous soil variables that drive root spread in the soil (e.g. soil water availability) may have great potential for providing spatial soil information cost-effectively (Malone, 2013). RF was conceived to produce accurate predictions that do

not overfit the data (Breiman, 2001), it is more powerful than classical spatial interpolation methods (e.g. regression tree, universal kriging, cubist; Liess et al., 2012) and more interpretable than other machine learning techniques, such as neural networks (Prasad et al., 2006). The use of these techniques in environmental studies, although growing, is still poor.

The aim of this paper is to quantify the potential of pioneer herbs against shallow landslides and erosion in temperate humid climates and identify key plant information to aid species selection for slope stabilisation. To do so, we follow a step by step journey from the study of the climate, soil and the root spread of three native perennial herbs growing on a landslide-prone slope in Northeast Scotland, to the verification of our revised spatially distributed eco-hydrological model; testing whether root spread information can be provided cost-effectively in temperate humid climates. The retrieved information on root spread is then used to evaluate the pioneer herbs' slope's topmost horizons stabilisation potential using a limit equilibrium method, which outcome will contribute to shed light on key plant-related data for effective plant selection against shallow landslides and erosion.

2. Materials & Methods

2.1. Study site

The study site lies within Catterline Bay, Northeastern Scotland, UK (WGS84 Long: -2.21 Lat: 56.90; Fig. 1), a region with mean annual temperature of 8.02 ºC and mean annual rainfall of 1232 mm (UK Met Office, 2015); constituting a humid temperate climate site (Cfc: subpolar oceanic climate; Köppen, 1884). The precipitation is

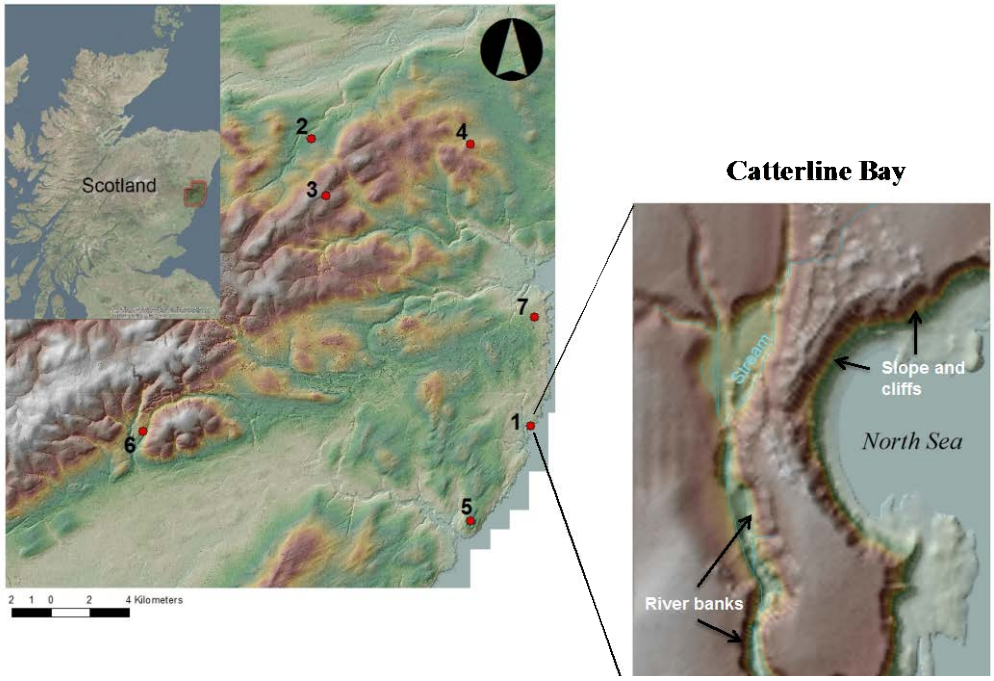

Figure 1. Study site location, topography, and location of the meteorological stations considered in this study. 1: Catterline; 2: Durris; 3: Mongour; 4: Netherley; 5: Inverbervie; 6: Fettercairn; 7: Stonehaven. Sloped terrain, cliffs and inclined riverbanks shown in darker shade/colour.

178 characterized by frequent, low-intensity rainfall events, while heavy storms seldom
179 occur. The topography of the study site is dominated by sloped (25-50º) terrain and
180 cliffs ending up into the sea, combined with a flatter inland area that is crossed by a
181 small stream that leads to the formation of inclined river banks (Fig. 1). Shallow (ca.
182 600 mm) and well-drained soils can be found within the study area resting on top of
183 sedimentary bedrock (i.e. conglomerate; BGS, 1999). The vegetation cover is
184 dominated by herbaceous weeds and grasses, riparian trees and agricultural crops of
185 wheat and barley. The sea has a limited influence on the vegetation as south-westerly
186 winds prevail. Different soil mass wasting episodes (landslides and erosion) have
187 been reported on the site in the past (e.g. Kincardineshire Observer 11/4/2013),
188 mainly associated with prolonged rainfall periods. The failure zones are easily
189 identifiable, presenting exposed bare ground or areas of sparse vegetation
190
191 2.2 Parameterisation

The parameterisation process was carried according to the diagram shown in Fig. 2 in order to identify and quantify the studied systems' elements governing plant root spread and feed a model aiming at providing root spread information in temperate humid climates (i.e. root profile distribution model, RPDM; see 2.3).

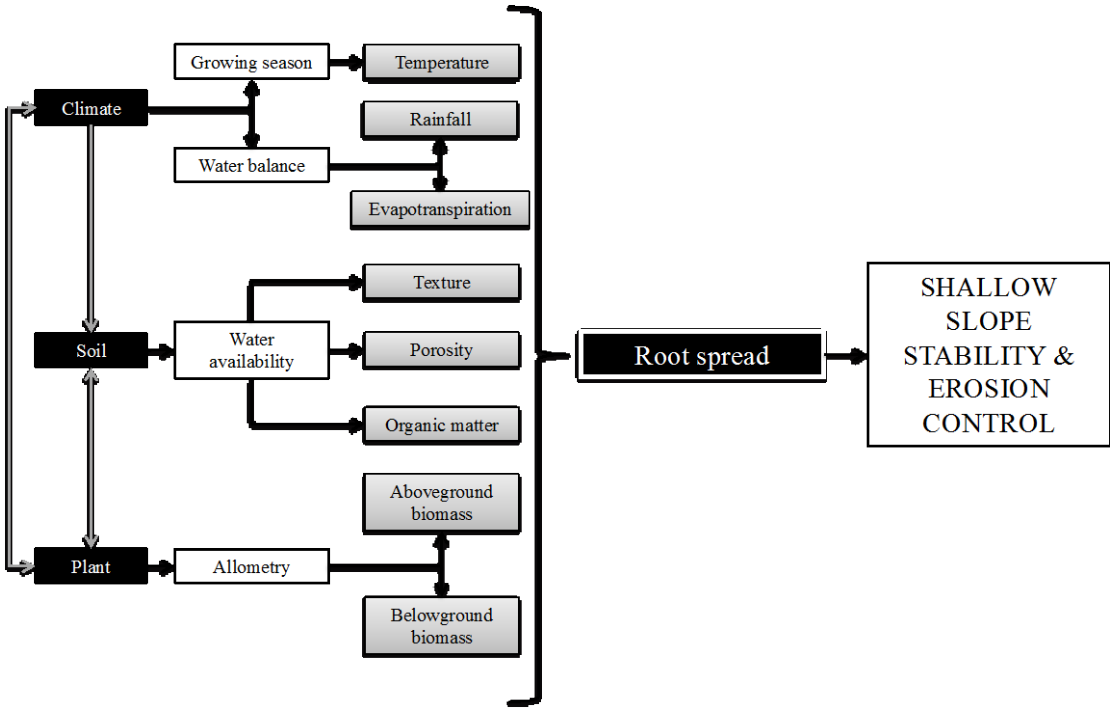

Figure 2. Arrow diagram showing the relationship between the considered compartments (black boxes) and parameters/variables (grey boxes) describing the root spread. Gray arrows indicate interactions between the compartments forming the ecosystem under study.

2.2.1 Climate parameters

Two types of climate data sets were employed: 1) short-term meteorological time series from a meteorological station located at the study site (2012-2014; vor de Porte, 2015; Fig. 1; Point 1) 2) long-term meteorological time series belonging to 6 different weather stations located within the region of the study site (1996-2014; UK Met Office, 2015; Fig. 1; Points 2 to 7).

The growing season duration was determined according to the growing degree-days (GDD) approach (e.g. McMaster & Wilhelm, 1997). We assumed that the growing season started once the cumulative GDD reached 200ºC, and that root growth was inhibited when the daily air temperature was below 5ºC (Alvarez-Uria and Körner, 2007). The duration of the growing season was estimated for each station and year and then it was averaged for the considered time series.

The probability distribution of the rainfall intensity for each growing season was assessed by estimating and plotting its kernel density (Parzen, 1962) in R 3.1.2 (R Development Core Team, 2014). Then, the rainfall parameters λ_o (i.e. frequency of rainfall events) and α (i.e. mean rain intensity) were estimated for each growing season as indicated in Preti et al. (2010). Both parameters, λ_o and α, were averaged over the considered time series and compared against the values obtained at the study site's station prior being used as input into RPDM (see 2.3). The mean evapotranspiration rate (T_p (mm d^{-1})) over the growing season was estimated with Priestly & Taylor (1972) equation and the extension proposed by Savabi et al. (1989) considering a broad-leaf vegetation cover (*LAI*: 3.48, Deguchi et al., 2006; aboveground biomass (M_a): 6140 g m^{-2}, Nunes et al., 2013).

2.2.2 Soil parameters

Undisturbed soil core samples from the uppermost 150 mm were collected at 30 random locations within the study site using an aluminum core sampler of 95 mm (inner diameter) and 150 mm (height). The soil samples were oven-dried at 110ºC over 24 hours to calculate the dry bulk density and porosity; assuming a soil particle density of 2.65 g cm^{-3} (Head, 1980). The soil particle size distribution was determined

by the dry sieving method and by the hydrometer method for the coarse (i.e. gravel and sand) and the fines fraction (i.e. silt and clay), respectively (BS 1377 Part 2:1990). Soil organic matter content was estimated through the loss on ignition method (Schulte and Hopkins, 1996). Soil saturated hydraulic conductivity was measured at 5 different locations with a constant head Guelph permeameter (Reynolds and Elrick, 1990). The former soil parameters were used to determine the soil's field capacity (θ_{fc}) and wilting point (θ_{wp}) by means of pedotransfer functions (Toth et al., 2015). The mean θ_{fc} and θ_{wp} values between the sampled points was employed as input into RPDM (see 2.3).

2.2.3 Plant parameters

Three different dominant species of perennial pioneer herbs were selected (Table 1) for parameterisation. All of them are native species that are well distributed over the entire UK, generally colonizing disturbed grounds (Perring and Walters, 1982). Plant sampling was carried at the height of the 2014's growing season (i.e. late July-early August) in which ten to eleven individuals of each species were sampled at random locations within the study site. Each plant individual was carefully excavated by hand without separating the above and belowground parts. In addition, to quantify the plant cover in terms of the aboveground biomass and the abundance of the selected plant species, twenty-five 1 m^2 quadrants were randomly sampled within the study site (USDA-NRCS, 1997).

Table 1. Studied herbaceous plant species.

Species	Family	Common name
Erigeron acris L.	Asteraceae	Blue fleabane
Rumex obtusifolius L.	Polygonaceae	Broad-leaved dock
Silene dioica Clariv.	Caryophyllaceae	Red campion

Each plant individual was clipped 2 millimetres above the collar with precision scissors to separate the above from the belowground part. The biomass of the above and belowground plant parts was determined after oven drying at 70ºC for 48 hours. The relationship between above and belowground parts (i.e. plant allometry) was evaluated through the implementation of exponential regression models in R 3.1.2, assuming a power-law relationship between both plant vegetative parts (WBE model; West et al., 1997; Cheng and Niklas, 2007) of the form $M_a = \beta M_r^{\alpha'}$, where M_a and M_r are the above and belowground biomass (g), respectively, β is the allometric normalization constant.

2.2.4. Root spread parameters

To estimate the root cross-sectional area with soil depth (i.e. rooted soil), the root diameters (d_i) for each depth interval were summed up and the area was then calculated as $A_i=\pi(\Sigma d_i/2)^2$, assuming that the soil-rooted area approaches a circumference at every considered depth and that fine roots are randomly distributed within. The average of all observations at every depth for each plant species were considered, to which an exponential regression model was fitted in R 3.1.2. The proportion of root-reinforced soil (i.e. root area ratio; *RAR*) was then calculated as $RAR(z)=A_i(z)/A_{soil}$. The mean rooting depth (b) was estimated as the average of the total rooting depth of all individuals per species divided by 3 (Laio, 2006). The root cross-sectional area at the ground level (Ar_o) was assessed like A_i but considering the root diameters at the root collar.

2.3 Root profile distribution model (RPDM) for temperate humid climates.

282

283 2.3.1. Model description

284

285 The eco-hydrological model RPDM for temperate humid climates was based on
286 Laio´s et al. (2006) model concept for the determination of the mean rooting depth (*b*)
287 at the plant community level for water-limited ecosystems. The former model (Laio et
288 al., 2006) estimates *b* (mm) as a function of the long-term water balance in the soil by
289 considering the ratio between the incoming water (i.e. rainfall) to the soil's available
290 water content (AWC) to plants, where AWC is in turn constrained by the atmospheric
291 water demand during the growing season - i.e. $b=\alpha/n(\theta_{fc}-\theta_{wp})(1-\alpha\lambda_o/T_p)$.
292 Contrariwise, we assumed herein that water income is no longer a limiting resource in
293 the soil profile for root system spread as, in temperate humid climates, precipitation
294 tends to be plentiful while evapotranspiration, or atmospheric water demand, is kept
295 at relatively low level (Allen et al., 1998). Therefore, we simplified Laio's analytical
296 model by considering that all the soil's incoming water would potentially be available
297 to plants. Hence, the mean rooting depth was estimated as:

$$b = \frac{\alpha}{n(\theta fc - \theta wp)} \qquad \text{(Eq. 1)}$$

298 where α is the mean rainfall intensity per event (mm/event) over the growing season
299 (see 2.2.1), and $n(\theta_{fc}-\theta_{wp})$ is the soil's available water content (AWC) to plants, being
300 n is the soil porosity (unitless), θ_{fc} is the soil's volumetric moisture content at field
301 capacity and θ_{wp} the soil's volumetric moisture content at wilting point (see 2.2.2).
302 Therefore, the mean rooting depth (*b*) would be just constrained by the soil
303 hydrological properties and fostered by the mean rainfall intensity during the growing
304 season (α). With this, it is also assumed that, according to hydrotropism principles

(e.g. Tsutsumi et al., 2003), the extent to which water can infiltrate in the soil profile is key to determining the extent of root profiles (Laio et al., 2006) and that evapotranspiration does not limit the availability of water to plants in temperate humid climates. Having estimated *b*, the soil depth at which the 95 % (i.e. z_{95}) of the roots can be found can be calculated as $z_{95}=3b$ (Laio et al., 2006).

The root distribution profile, or root spread, was considered to decrease exponentially with the soil depth (z); assuming that the probability distribution of the rainfall intensity was also exponential (Laio et al., 2006; see 2.2.1) and portrayed by $Ar(z)=Ar_o\exp^{-z/b}$ (Preti et al., 2010). Where $Ar(z)$ is the root cross-sectional area with soil depth (mm^2), Ar_o is the root cross-sectional area at the ground level (mm^2), z is the soil depth (mm) and b the mean rooting depth (mm). Assuming a conical shape root system, Ar_o was estimated from the plant aboveground biomass (M_a), allometric parameters (β and α'; see 2.2.3), the mean rooting depth (b) and root mass density (ρ_r) ($Ar_{o=}\ \beta M_a^{1/\alpha'}\ /\ b\rho_r$; Preti et al., 2010). Eventually, the root area ratio ($RAR(z)$) was estimated (see 2.2.3) .

2.3.2. Model quality

The goodness of fit of RPDM was quantified through the estimation of the coefficient of determination (R^2) by subtracting from 1 the quotient between the residual (i.e. difference between observed and predicted values) sum of squares and explained sum of squares (i.e. $R^2=1-SS_{res}/SS_{obs}$; e.g. Bivand et al., 2008). In addition, statistically significant differences between observed and regressed values for the parameters Ar_o and b were assessed with the chi-square (χ^2) test at the 95% and 99% confidence intervals in R 3.1.2.

330

331 2.3.3. Model sensitivity

332

333 The sensitivity of RPDM was analyzed with the One-factor-At-a-Time approach
334 (OAT; Daniel, 1973), considering the mean root cross-sectional area as the model
335 output. The 9 independent model parameters (Table 2) were considered and their base
336 value was varied ±20% to account for natural variability. One model run was carried
337 for each parameter value change (i.e. 18 model runs in total). The parameter change
338 that generated the greatest output variation with respect to the original model run was
339 kept for the estimation of the sensitivity index (SI) and the percentage of variation
340 (PV) (Felix & Xanthoulis, 2005). Finally, the effect of the most sensitive parameters
341 on the root distribution profiles was evaluated and discussed.

342 Table 2. RPDM's independent parameters considered within the sensitivity analysis.

Symbol	Parameter
M_a	Plant's aboveground biomass (g)
α'	Allometric power-law parameter
β	Allometric parameter
ρ_r	Root mass density (g cm^{-3})
OM	Soil's organic matter content (%)
Silt	Soil's silt content (%)
Clay	Soil's clay content (%)
n	Soil porosity (unitless)
α	Mean rain intensity during growing season (mm H_2O/event)

343
344

345 2.3.4. Model expansion: spatially distributed RPDM

346

347 RPDM expansion was carried using the '*raster stack*' concept (a collection of raster
348 layers with the same spatial extent and resolution) of the R's package 'raster'
349 (Hijmans, 2014). Thus, we modeled a given soil column, of a pixel size area (i.e.
350 raster resolution), as the pool of superimposed raster pixels for a given XY coordinate

within a given raster stack (Fig. 3). The range of depths for a given soil profile was then portrayed by each layer in the stack; assigning the same z-value (depth) to every pixel belonging to the same stack layer. This approach makes also possible to assign different attributes to each layer in order to mimic the features of different soil horizons. However, isotropic soil profiles were considered herein for the sake of simplicity.

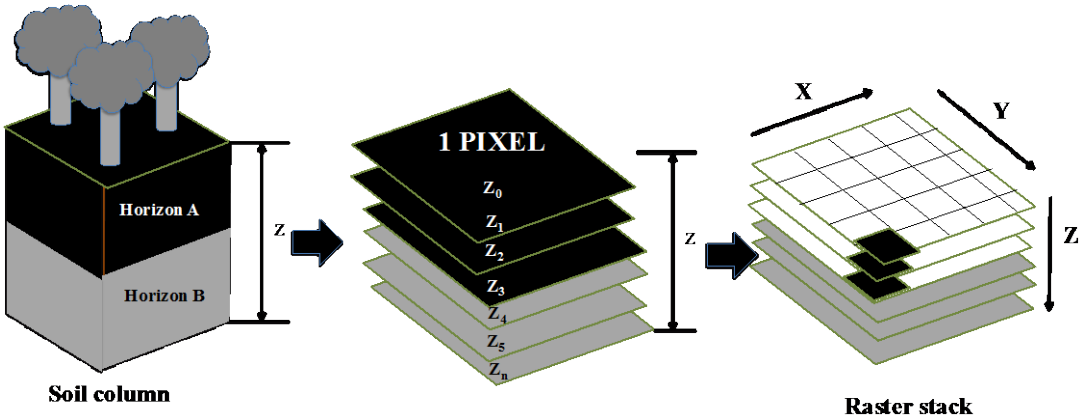

Figure 3**.** Illustration of how RPDM-3D models a given soil column. Each pixel portrays a different soil column of area the pixel size. Each soil column may have a custom number of layers, each portraying a different soil depth (z_n) or additional customizable soil attributes that vary with soil depth. The pool of soil layers is combined in a *raster stack* formed by the superposition of raster layers.

The spatially distributed RPDM was tested on our study site (i.e. Catterline bay; Fig. 1), where the root spread and, its corresponding effect on slope stability (see 2.4), were retrieved from 4 randomly selected pixels. Soil spatial inputs to RPDM were obtained by spatially interpolating the measured soil parameters (see 2.2.2). The spatial interpolations were carried with the machine learning algorithm 'Random Forest' (RF) (Breiman, 2001) using terrain attributes (i.e. slope, aspect, curvature and shade) and plant cover as environmental spatial covariates (Table 3); following the principles of the '*scorpan*' approach (Jenny, 1941). The terrain attributes were derived from a 2m digital surface model (DSM) (GetMapping, 2014) using the 3D Spatial Analyst package of ESRI ArcGIS 10.1. RF was implemented using the R package *randomForest* (Liaw and Weiner, 2002) in R 3.1.2. RF's outcome was

validated using a random-hold back, or bootstrapping method (Efron, 1979), through the estimation of R^2 as indicated in 2.3.2.

Table 3. Soil spatial prediction formulas and environmental covariates implemented with the RF algorithm for each of the considered soil spatial variables.

Spatial variable	Formula and environmental covariates
Soil sand content (%)	Sand=Slope+Aspect+Curvature+Plant cover
Soil fines content (%)	Fines=Slope+Aspect+Curvature+Plant cover
Soil silt content (%)	Silt=Slope+Aspect+Curvature+Plant cover
Soil clay content (%)	Clay=Fines-Silt
Soil organic matter (%)	OM=Slope+Aspect+Curvature+Plant cover+Sand
Dry bulk density (g/m^3)	Bulk= Slope+Aspect+Curvature+Plant cover+Sand+Fines+OM
Plant biomass (g/m^2)	Biomass=Slope+Aspect+Curvature+Shade+Sand+Fines+OM+Plant cover

2.4. Root mechanical effect against shallow landslides

To assess the soil-root mechanical reinforcement effect against shallow landslides, the retrieved root spread information was employed to estimate the apparent root cohesion ($c_R(z)$) with the widely used simple perpendicular model (SPM; Waldron, 1977; Wu et al., 1979), which requires a measurement or estimation of the root area ratio (*RAR*(z)) and the mean root tensile strength (T_r) as input. $c_R(z)$ was directly added to the resisting forces (Wu et al., 1979; Ekanayake and Phillips, 2002; Norris et al., 2008) for the estimation of a factor of safety (FoS(z)= $c_R(z)$+*resisting*(z)*/driving*(z)) using an infinite slope limit equilibrium method (LEM; Lu and Godt, 2008).The former LEM method (Lu and Godt, 2008) does not require assuming the location of a particular critical plane of failure. Instead, the latter is detected in light of the soil's hydro-mechanical properties and conditions. However, a lower boundary for the system under study was arbitrarily set at 500 mm below the ground level (b.g.l), far below the expected reach of the herbaceous root systems in order to avoid edge effects.

393 The values of T_r were as per the reported values in literature (i.e. T_r^{herbs}=3.73 MPa,
394 Comino et al., 2010). RAR(z) for each studied herb species was derived from the total
395 aboveground biomass per unit area (M_a^T) using the plant cover and abundance (see
396 2.2.3) from the two quadrants where the selected species were the most abundant.
397 The studied species´ soil-root reinforcement was compared against the effect provided
398 by an oak tree (*Quercus robur* L.; T_r^{oak}= 8.00 MPa, Stokes et al., 2008; M_a=6300 g m^{-}
399 ^{2}, Nunes et al., 2013; α'=0.8 β=3.42, Cheng and Niklas, 2007) and bare soil. To stress
400 the soil-root reinforcement effect, cohesionless and hydrostatic soil conditions were
401 assumed.
402 Statistically significant differences between the treatments were evaluated with a
403 Kruskal-Wallis test among the winsorized means (Wilcox and Keselman, 2003) of
404 FoS trimmed at 20% and at the 95 and 99% confidence intervals.
405
406 3. Results
407
408 3.1. Parameterisation
409
410 3.1.1 Climate parameters
411
412 Climate parameterisation results (Table 4) show that the mean annual rainfall (R) for
413 the study site was the lowest of all considered stations (i.e. 565.13±46.89 mm) while
414 the annual evapotranspiration (ETP) was the highest (489.38±4.29 mm). All stations
415 presented higher R respect to ETP. The mean rainfall intensity per event (α) ranged
416 between 3.20 and 9.14 mm, belonging the lowest found to the study site. The growing
417 season duration would last from mid-late May to mid October for all considered

stations. The rainfall intensity density functions (Figure 4a) were exponential for the study site.

Table 4. Calculated climatic features and mean growing season duration (GSD) for each meteorological station. α: mean rainfall intensity per event±standard error; λ_o: frequency of rainfall event±standard error; R: mean annual rainfall±standard error; ETP : mean annual evapotranspiration±standard error.

Station	Distance (km)	Period	α (mm per event)	λ_o	R (mm)	ETP (mm)	GSD (day/month)
Catterline		2012-2014	3.20± 0.38	0.64± 0.02	565.13± 46.89	489.38±1 4.29	23/5 – 11/11
Durris	19.6	1996-2014	5.33± 0.32	0.54± 0.02	1020.15± 40.35	461.69± 10.77	11/5 – 14/10
Mongour	15.8	1996-2014	9.86± 1.83	0.72± 0.05	1011.52± 113.01	468.08± 8.80	29/5– 7/10
Netherley	14.9	1996-2013	5.07± 0.30	0.64± 0.02	1022.22± 88.39	461.54± 10.26	13/5 – 16/10
Inverbervie	5.8	1997-2007	9.14± 0.72	0.66± 0.02	1905.74± 153.41	-	-
Fettercairn	19.9	1996-2014	4.66± 0.27	0.62± 0.01	971.31± 48.35	-	-
Stonehaven	5.7	1996-2013	3.76± 0.29	0.57± 0.02	747.00± 52.15	438.19± 24.41	17/5-23/10

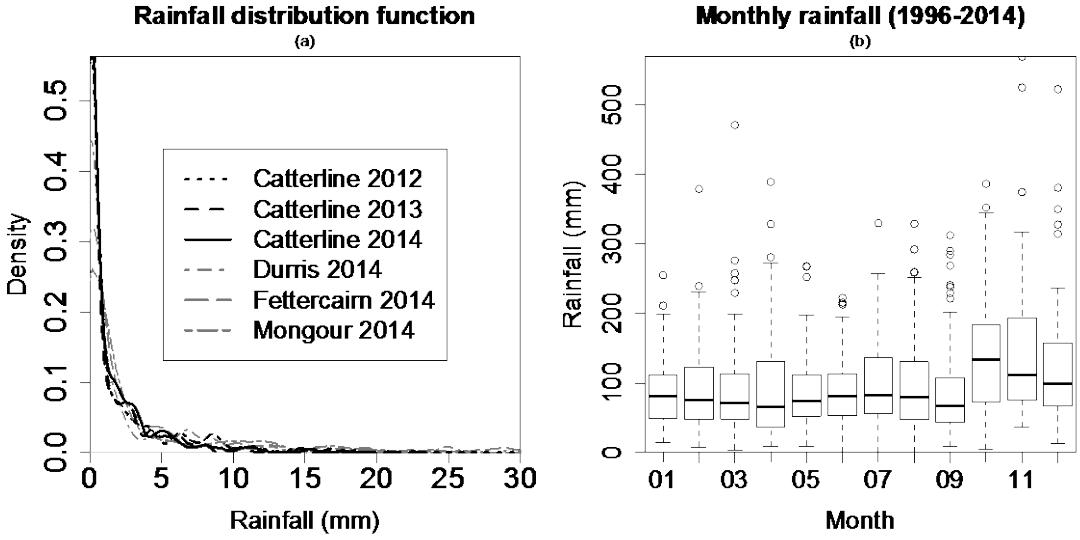

Figure 4. a) Rainfall intensity probability distribution functions for the study site (2012-2014) and a three other meteorological stations for the year 2014 b) Monthly rainfall distribution throughout the year averaged per meteorological station between all the studied time series, where the bottom and top of the boxes represent the first and third quartiles, respectively, the band inside the box represents the median, and the points represent outliers from all the studied time series.

3.1.2 Soil parameters

The soil parameterisation results (Table 5) indicated that relatively porous, silty sands (Craig, 2004), with high organic matter content (Urbano, 1992) and good drainage conditions (Head and Epps, 2011) can be found within our study site..

Table 5. Measured mean value for each of the considered soil variables averaged between the sampling points and standard errors. OM: organic matter content; $\rho_{b:}$ soil bulk density; n: soil porosity; Ks: saturated hydraulic conductivity; θ_{fc}: volumetric moisture content at field capacity; θ_{wp}: volumetric moisture content at wilting point.

Sand (%)	Silt (%)	Clay (%)	OM (%)	ρ_b (g/cm^3)	n	Ks (m/s)	θ_{fc}	θ_{wp}
74.97	2.87	1.60	5.57	0.86	0.68	5.82e-5	0.23	0.09
±2.47	±0.19	±0.12	±0.65	±0.06	±0.02	±1.43e-5	±0.003	±0.001

3.1.3 Plant parameters

Results from the plant parameterisation (Table 6) show that the aboveground dry biomasas (M_a), at the individual level, and for the three studied herb species, ranged between 14.20±1.45 g (*E. acris*) and 27.65±8.66 g (*R. obtusifolius*). The belowground dry biomass (M_r), however, ranged between 1.65±0.71 g (*S. dioica*) and 13.36±4.05 g (*R. obtusifolius*). The plant abundance in the study site (*A*; Table 6) varied between 21.50 % (*S. dioica*) and 10.87 % (*E. acris*).

The allometric parameters (α' and β; Table 6) were different for all the studied herbs and only *Erigeron acris* presented an exponential allometric relationship between M_a and M_r (α'=0.43; β=9.06; R^2=0.65; Figs. 6d-f) while the other two species shown a linear relationship (Figs. 6d-f) with a higher goodness of fit (i.e. $R^2 \geq 0.95$; Table 6).

3.1.4 Root spread parameters

The measured mean rooting depth (Table 6) spanned from 21.21±3.52 mm (*S. dioica*) to 45.45±2.82 mm (*R. obtusifolius*). The species that presented the largest root cross-sectional area at the ground level (Ar_o) was *Rumex obtusifolius* (747.08±301.58 mm^2).

Table 6. Quantified (Q) and modelled (M) allometric and root spread parameters and variables. M_a: aboveground plant biomass; M_r: belowground plant biomass; α': allometric power exponent; β: allometric normalisation co
cross-sectional area at the ground level; b: mean rooting depth; RAR: root area ratio; R^2: coefficient of determination; N: sample size; A: plant species abundance; M_a^T: total plant aboveground biomass per m^2. RPDM models
mean plant biomass between all studied individuals, and study site's climate input and averaged climate input from the other 6 stations, respectively. RPDM models C and D employ total plant biomass, and study site's c
averaged climate input from the other 6 stations, respectively. Q: mean ± standard error

Species	Type	Model	M_a (g)	M_r (g)	α´	β	Ar_o (mm^2)	b (mm)	RAR (%)[a]	R^2	N	A(%)	M_a^T ($g\ m^{-2}$)[b]
E. acris	Q		14.20±1.45	3.14±0.67	-	-	178.33±55.58	40.74±5.82	$3.68x10^{-3}$±$5.52x10^{-5}$		10	10.87±0.79	325
	M	Allometric	-	-	0.43	9.06	-	-	-	0.65	-	-	-
	M	Regression	-	-	-	-	125.23	45.91	-	0.96	-	-	-
	M	RPDM A	-	-	-	-	78.55	45.48	-	0.74	-	-	-
	M	RPDM B			-	-	41.03	87.08	-	0.43	-	-	-
R.obtusifolius	Q		27.65±8.66	13.36±4.05			747.08±301.58	45.45±2.82	$1.88x10^{-2}$±$2.30x10^{-4}$		11	20.41±1.58	1400
	M	Allometric	-	-	0.99	2.13	-	-	-	0.95	-	-	-
	M	Regression	-	-	-	-	566.15	56.54	-	0.93	-	-	-
	M	RPDM A	-	-	-	-	366.10	45.48	-	0.61	-	-	-
	M	RPDM B	-	-	-	-	191.24	87.07	-	0.32	-	-	-
S. dioica	Q		16.74±7.61	1.65±0.71	-	-	541.13±136.53	21.21±3.52	$1.79x10^{-2}$±$4.15x10^{-4}$		11	21.50±2.12	325
	M	Allometric	-	-	1.021	10.07	-	-	-	0.98	-	-	-
	M	Regression	-	-	-	-	443.81	35.52	-	0.99	-	-	-
	M	RPDM A	-	-	-	-	45.20	45.48	-	0.19	-	-	-
	M	RPDM B	-	-	-	-	23.61	87.08	-	0.19	-	-	-
	M	RPDM C	-	-	-	-	473.30	45.48	-	0.83	-	-	-
	M	RPDM D	-	-	-	-	247.23	87.08	-	0.66	-	-	-

[a]RAR: mean percentage ± standard error of all the studied plant individuals between the depths 0-250 mm for E.acris, 0-200 mm for R. obtusifolius and 0-170 mm for S.dioica.

[b]M_a^T: mean of the total aboveground biomass found at the two quadrants in which the considered plant species was the most abundant.

The mean RAR between the considered depths (Table 6) ranged between $3.68 \times 10^{-3} \pm 5.52 \times 10^{-5}$ % and $1.88 \times 10^{-2} \pm 2.3 \times 10^{-4}$ % for *E. acris* and *R. obtusifolius*, respectively.

3.2 Root systems spread and RPDM

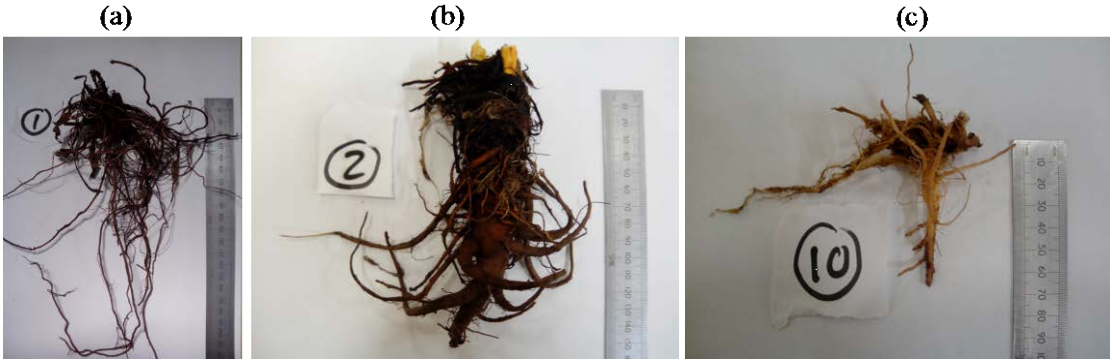

Figure 5. Selected root systems of a) Erigeron acris b) Rumex obtusifolius c) Silene dioica

The root systems (Fig. 5) for the three studied species (Table 1) presented clear morphological differences. Regarding the root spread (Figs. 6a-c), the three species shown a decreasing exponential profile distribution with soil depth to which an exponential regression model was fitted with a goodness of fit (R^2) above 0.9 in all cases (Table 6). All root systems investigated were distributed within the uppermost 300 mm of the soil profile, with the deepest root system belonging to *Rumex obtusifolius* (Fig. 6b)

RPDM predictions for the root spread parameters, b and Ar_o, and their respective predictive capacities, are gathered in Table 6. RPDM predicted values for both parameters that did not significantly differ (χ^2=1.66, df=2; χ^2=1.34, df=2) from the observed and regressed counterparts (Table 6) when the study site´s meteorological inputs were employed.

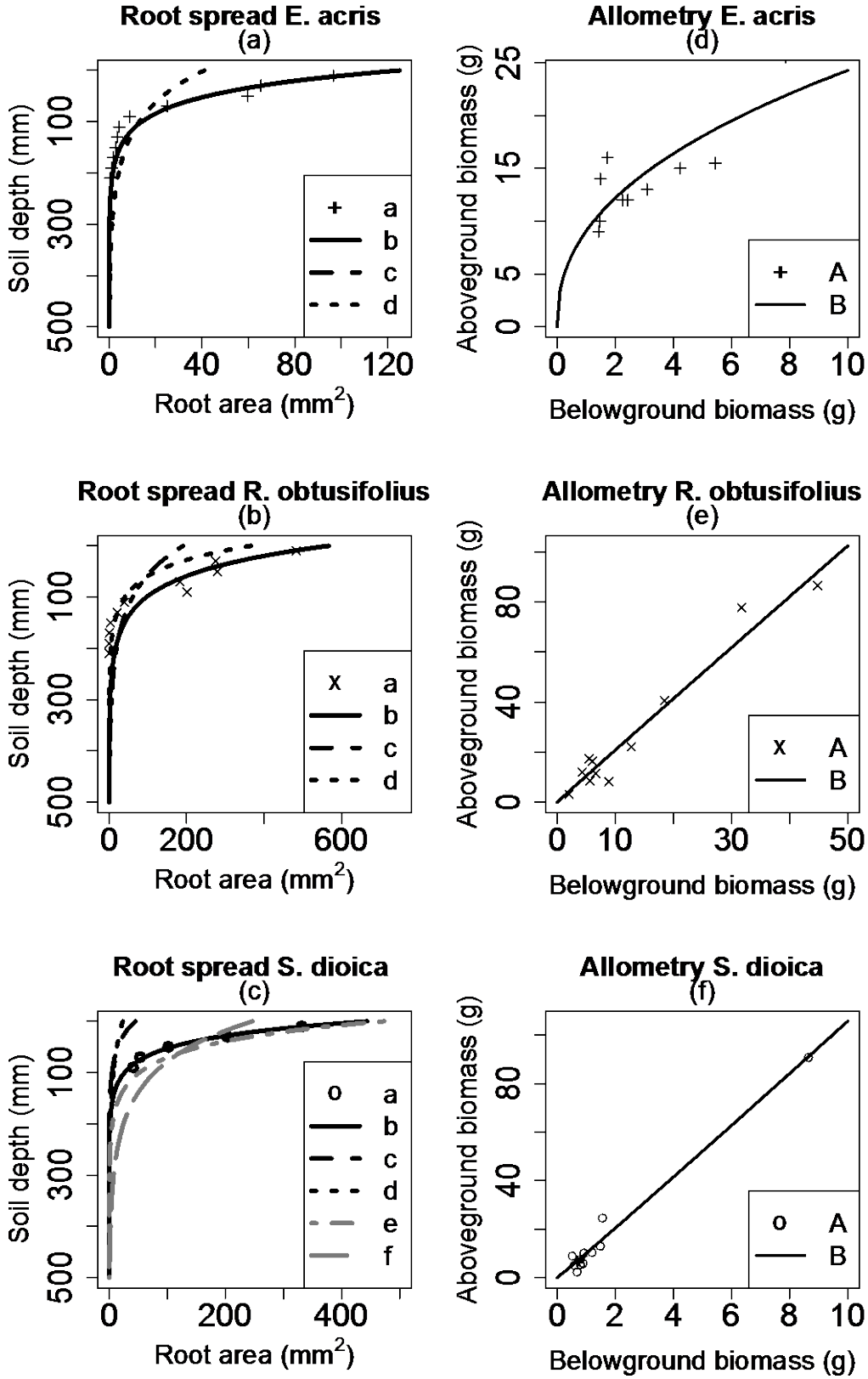

Figure 6. a-c) Measured and predicted root spread for d) *E. acris* e) *R. obtusifolius* f) *S. dioica*, where a: observed values; b: regressed values; c: predicted values from RPDM using study site's climate input; d: predicted values from RPDM using averaged climate inputs from the other 6 weather stations; e and f: predicted values from RPDM using the total biomass of all studied individuals of *S. dioica* and, study site's climate input and rest of the stations input, respectively d-f) Measured allometric relationships between aboveground and belowground vegetative parts for a) *E. acris* b) *R. obtusifolius* c) *S. dioica*, where A: observed values; B: fitted values.

487 3.3 Sensitivity analysis of RPDM

488

489 Sensitivity analysis outcomes for RPDM are presented in Figs. 7a-d, being the
490 allometric parameter β (PI=68 %; SI=-2.28), the plant's aboveground biomass (M_a;
491 PV=52.8 %; SI=2.29) and the mean rainfall intensity during the growing season (α;
492 PV=30.22 %; SI=-1.18) the three most sensitive parameters upon predicting root
493 spread.

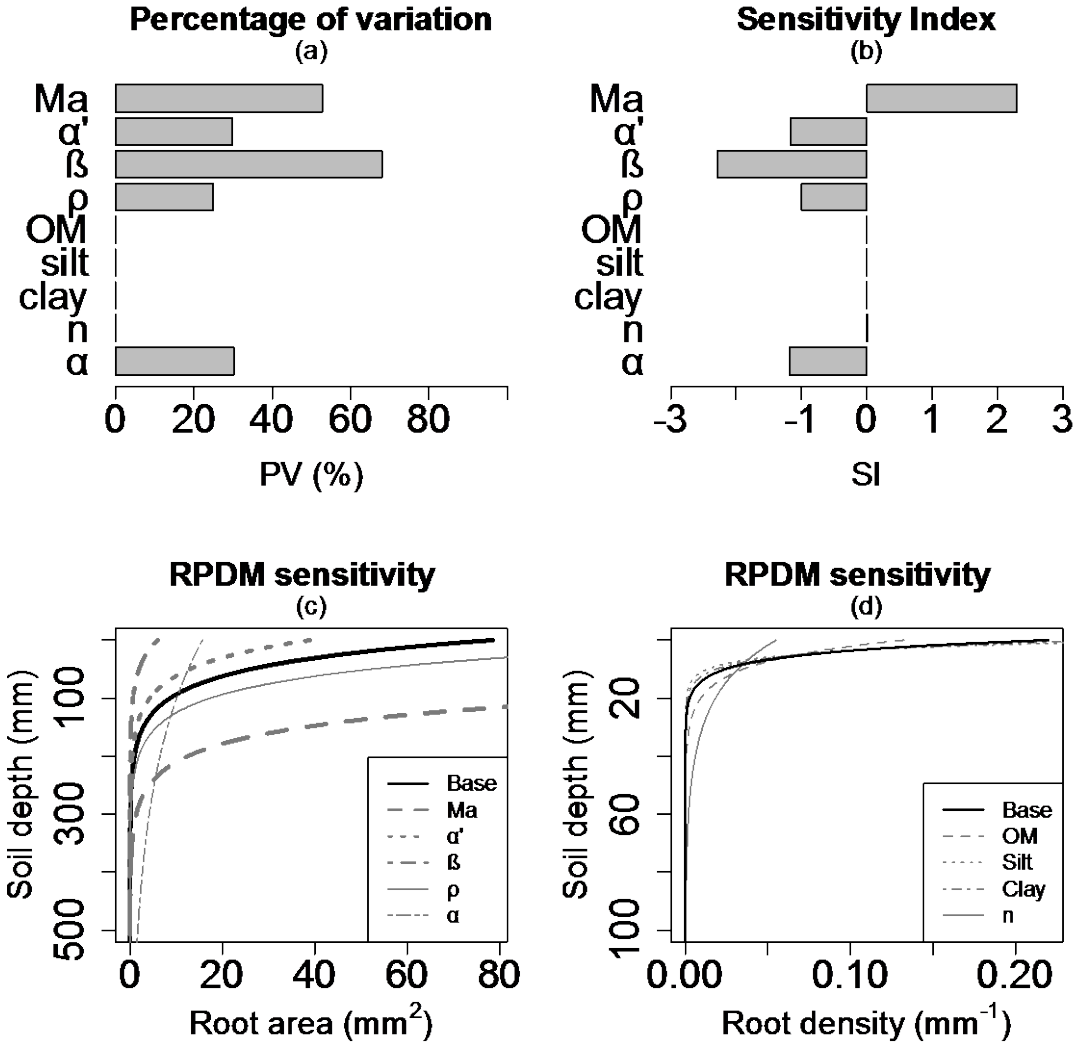

494 Figure 7. Sensitivity analysis outcome for RPDM a) Percentage of variation (PV) b) Sensitivity index (SI) c) RPDM output for the base model run and after applying value changes to the most sensitive parameters respect to the base model run: M_a: aboveground biomass (g) (base*3): α': power-law allometric parameter (base*3); β:
495 allometric constant (base*3); ρ: root mass density (g cm^{-3}) (base*0.5); α: rainfall intensity (mm H_2O/event) (base*5) d) Effects of soil´s model parameters on the root density distribution function ($r(z)=b^{-1}e^{-z/b}$): OM: organic
496 matter (%) (base*0.1); Silt : soil's silt content (%) (base*10); Clay: soil's clay content (%) (base*10); n: soil porosity (base*0.25).

3.4. Spatially distributed RPDM

3.4.1 Soil spatial interpolation

Spatial interpolation outcomes for the soil properties and plant biomass are shown in Table 7. The predictive capacity of the implemented RF algorithms (Table 3) for the soil texture (%Sand:R^2=0.94; %Fines:R^2=0.93) and soil organic matter (R^2=0.88) was high while it was relatively low for the plant biomass cover (R^2=0.31).

Table 7. Outcome from random forest (RF) spatial interpolations for each of the considered soil spatial variables. R^2: coefficient of determination; RMSE: root-mean-square-error.

Spatial variable	Variance explained (%)	R^2	RMSE
Soil sand content (%)	62.86	0.94	11.82
Soil fines content (%)	66.8	0.93	54.32
Soil silt content (%)	34.1	0.66	57.02
Soil organic matter (%)	42.78	0.88	1.11
Dry bulk density (g/m^3)	53.16	0.81	0.32
Plant biomass (g/m^2)	33.59	0.31	841.51

3.4.2 Spatial prediction of root spread

The outcome from the spatial prediction of the root spread is shown in Fig. 8 in terms of the rooting depth (i.e. z_{95} =3b; soil depth at which 95 % of the roots can be found) and in Fig. 9a in terms of the root profile distribution for 4 randomly chosen points (i.e. Points A, B, C and D; Fig. 8). Results indicated a maximum herbs rooting depth of ca. 200 mm on flat zones while steeper terrain presented shallower root depths (ca. 100-125 mm).

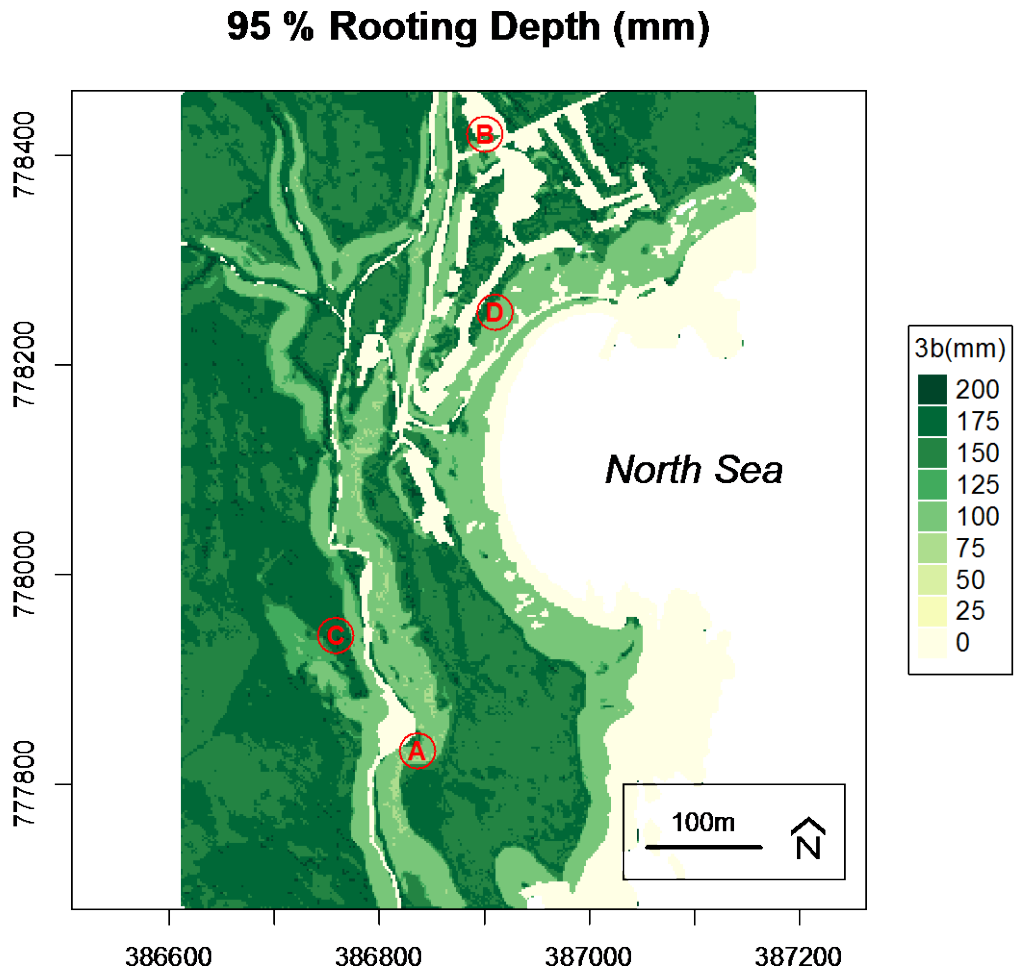

Figure 8. RPDM spatial predictions for the rooting depth (mm) at which 95 % of the root system can be found (i.e. z_{95}=3b) in the soil in our study site, and points A, B, C and D at which root reinforcement profiles were assessed.

3.5 Mechanical effect of root spread on slope stability

The mechanical effect of root spread on slope stability (Fig. 9b) for each randomly selected point within the study area (i.e. Points A, B, C and D; Fig. 8) was limited to the topmost soil (i.e. 0-200 mm) and showed differences in light of root spread differences (Fig. 9a) provided by soil spatial properties differences. The predicted apparent root cohesion (Fig. 9c) and its subsequent mechanical effect on slope stability (Fig. 9d) for the 3 studied species and for the 2 additional treatments (i.e. oak tree and bare soil) pointed that it was *Erigeron acris* the most effective herb species

from the soil-root reinforcement point. However, no statistically significant differences were found between the 5 considered treatments (χ^2=7.82, df=4).

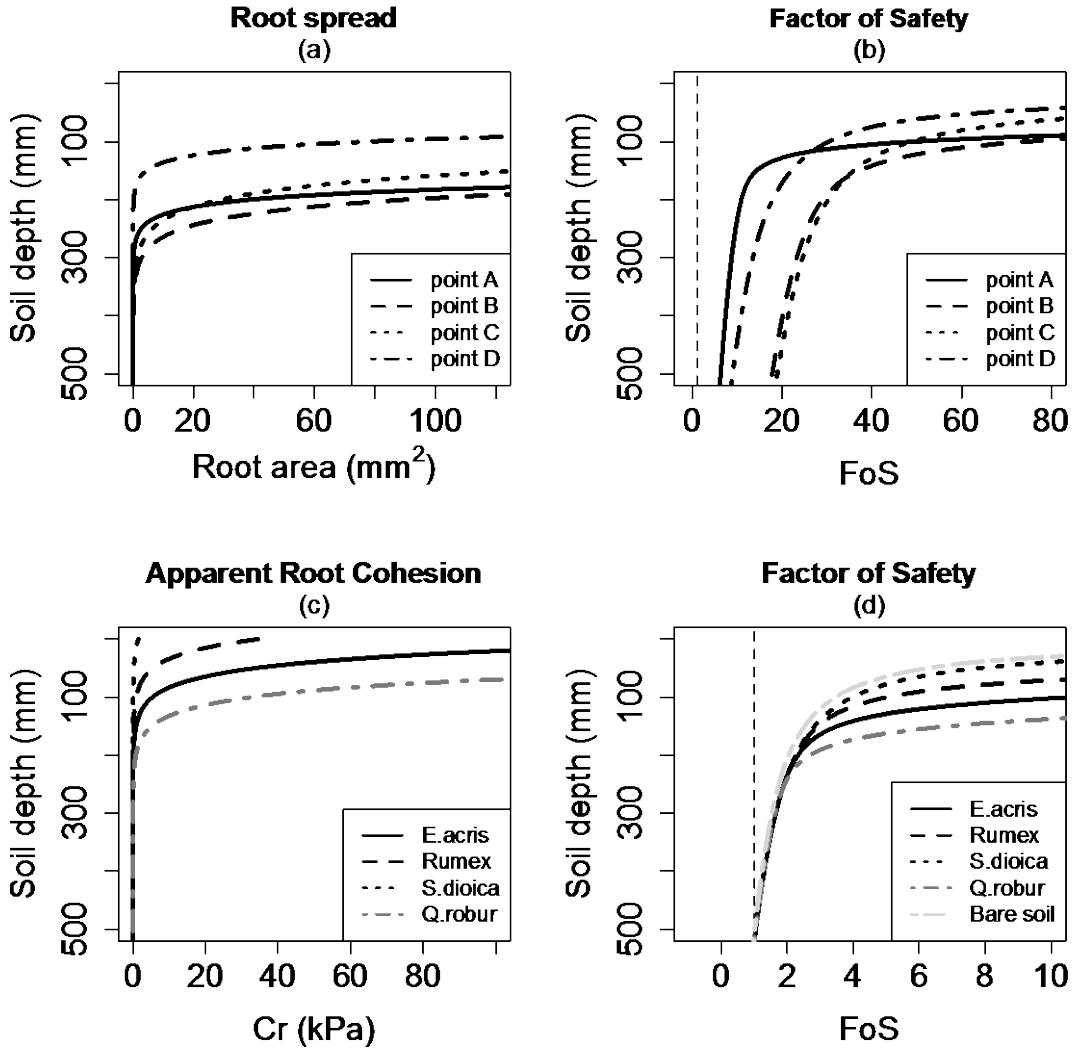

Figure 9. a) Predicted root spread in terms of the root cross-sectional area (*Ar*) at four different points (i.e. pixels) within the study site and indicated in Fig. 7 b) Predicted Factor of Safety (FoS) profiles at the four points indicated in Fig. 7 c) Predicted apparent root cohesion profiles assuming fully-vegetated unit area of ground by each of the considered plant species d) Estimated Factor of Safety (FoS) profiles for each considered vegetation cover and bare soil, where FoS < 1 = slope failure and Fos >1 = slope stable.

4. Discussion

4.1 Climate parameters

All the stations presented a similar, and lower, *ETP* with respect to *R* (Table 4), representative of humid climates (UNEP, 1992), confirming that Laio´s original

541 model (Laio et al., 2006) is not applicable to our study area and supporting the need
542 of modification for our study site. In addition, the shape of the rainfall intensity
543 distribution function (Fig. 4a) was exponential for all the studied rainfall time series
544 belonging to our study site. Hence, according to Laio's (2006) original model, the
545 root systems in our study region should be expected to be exponentially shaped;
546 supporting the assumption made in this regard (see 2.3.1).
547 In reference to the growing season duration (Table 4), only minor differences were
548 found between all the considered meteorological stations and with no summer
549 dormancy. The late start of the growing season in our study area compared to warmer
550 regions (e.g. Preti et al., 2010; Tron et al., 2014) would lead to a late start of the
551 vegetation activity that, for the case of annual herbs, would produce a negligible
552 effect on shallow soil instabilities until very late in the spring season. On the other
553 hand, rainfall events were evenly distributed over the entire year throughout the
554 considered time series (Fig. 4b). Consequently, the duration of the growing season
555 was not expected to have a significant impact on the RPDM predictions in this regard
556 (see 4.4). Nonetheless, in case of an uneven rainfall distribution throughout the year
557 (i.e. seasonal), an accurate determination of the growing season duration would be
558 paramount for a better prediction of the root distribution profiles (Tron et al., 2014).
559 Both the mean annual rainfall (R), as well as the mean rainfall intensity during the
560 growing season (α) were considerably lower in our study site than for the rest of the
561 stations (Table 4) which presented wetter conditions. As a result of this, and based on
562 RPDM formulation (see 2.3), shallower root systems would be expected in our study
563 site in comparison with sites closer to the other meteorological stations.
564
565 4.2. Soil parameters

The results from the soil parameterisation (Table 5) suggest that rainfall infiltration will not be constrained by the soil properties and the AWC to plants ($n(\theta_{fc}-\theta_{wp})$) will be adequate for the development of root systems in depth. According to this, we believe that rainfall infiltration will mainly be driven by gravity (i.e. producing a vertical flow) despite the terrain steepness (Lu and Godt, 2013). Although runoff will also be fostered by the topographical conditions once the topsoil moisture approaches saturation levels (Mein and Larson, 1973), on average (i.e. throughout the growing season) this will not affect significantly the water availability for root development (Tron et al., 2014). Additionally, lateral flow will not likely be produced until infiltrating water reaches the bedrock (Neitsch et al., 2011), which, presumably, is out of the root system's influence as root systems tend to be relatively shallow in temperate humid climates (Schenk and Jackson, 2002).

4.3 Root spread and plant parameters

4.3.1 Root spread

The obtained exponential root profiles (Figs. 6a-6c) validate the assumption of considering an exponentially shaped root distribution profile and corroborate Laio's notion (Laio et al., 2006) that the rainfall intensity distribution function largely determines the root system's shape in the soil profile. However, on an individual basis, it was observed that some profiles better resembled a gamma shaped distribution (unpublished data). Hence, local ecological factors other than rainfall distribution and water availability may have an influence on the shape of the root profile (e.g. Casper et al., 2003; Schenk, 2005).

All root systems just explored the uppermost soil profile (i.e. 0-300 mm b.g.l) and in depths depending on the plant biomass (Fig. 6a-c; Table 6). In the same line, it was also observed that the proportion of rooted soil (i.e. *RAR*) varied with plant biomass (Table 6, Figs. 6a-c); the higher the plant biomass the higher the root cross-sectional area in the topmost soil horizons. The fact that higher biomass plants tend to spread wider and deeper may be related to the plant's own stabilisation in the ground (Chiatante et al., 2003) or related to resources use efficiency and competition issues with other plant species (Schenk, 2005).

The values of root exploration depth were in good agreement with globally observed values for cool-temperate meadows (Schenk and Jackson, 2002; Yang et al., 2009), alpine herbs (Burylo et al., 2011), and for cool temperate ecosystems in general, where the upper 200 mm of the soil profile contains, on average, the majority of all roots (Schenk & Jackson, 2002). For the case of *Rumex obtusifolius*, its root distribution matched the observations gathered in Laan et al. (1989) for riparian ecosystems in the Netherlands. Our results were more realistic than the reported in the literature (Cannadell et al., 1996; Schenk and Jackson, 2005), where it was postulated that root systems could explore as much as 2 m depth of the soil profile for climate parameters matching our study site's which is not achieved even by woody plants in the UK (e.g. Nicoll & Amstrong, 1998; Crow, 2005). It is worth noting that shallow root systems were expected to be found as, indicated earlier (see 2.3.1), plant water availability will not be constrained in the topmost soil horizons in temperate humid climates. Nonetheless, it must be borne in mind that the whole root systems were excavated from their natural environment, and different records may be obtained with onsite measurement methods, such as the profile wall method (Böhm, 1979). Regarding the observed *RAR* values, these were in all cases lower than the values

indicated, for example, in Comino et al. (2010) for other herbaceous species at a hypothetical shear plane of 100 mm. This indicates that the approach employed herein for measuring the root cross-sectional area did not lead to overestimation of its value.

4.3.2 Plant parameters

Given that plant biomass had a significant effect on the root spread, the plant allometry or the relationship between above and belowground vegetative parts, was expected to be the key parameter for readily providing information on the root spread using less invasive sampling methods and to support decisions on plant selection for slope stabilisation.

As stated earlier (see 3.1.3), the three studied plant species showed different allometric relationships between their respective above and belowground vegetative parts (Figs. 6d-f). For the case of *Rumex obtusifolius* and *Silene dioica* a complete isometric relationship was found (Figs. 6e-f), as indicated by Niklas (2005) for the case of non-woody plant species. On the contrary, for the case of *Erigeron acris* an exponential relationship was found between the two vegetative parts (Fig 6d), which is not commonly observed in herbaceous plant species (Cheng and Niklas, 2007). The value of α' we recorded for *E. acris* was 0.43 (n=11, SE=0.103; Table 6) which compares to the value of ¾ in the original WBE model (West et al., 1997). This may be due to errors in the measuring technique (Enquist et al., 1998), or due to the limited sample size. On the other hand, although we did not log-transformed the considered variables (i.e. M_a and M_r), as it is normally the case in most biometrical studies (West et al., 1997), a clear allometric relationship was directly found using the untransformed variables and with an ordinary least squares regression (OLS); which

641 may be valid for plant species with lower biomass. In any case, the fitting parameters
642 β and α' differed across the three studied plant species, giving support to the idea of
643 'non-universal' scaling allometric parameters (Li et al., 2005). Nevertheless, it is
644 worth noting that the WBE general model (West et al., 1997; Enquist et al., 1998)
645 states that the scaling parameters are predicted to change in very precise numerical
646 ways attending to ontogeny or differences in ecological settings. Therefore, further
647 research is recommended to clarify the sensitivity of β and α' to different ecological
648 factors (e.g. light, nutrients, water, topography) and shed light on the employability of
649 these plant parameters upon plant selection for eco-engineering purposes.
650
651 4.4 Root profile distribution model (RPDM)
652
653 4.4.1 Model predictions and quality
654
655 The predictive capacity of RPDM was shown to be very high in all cases (Figs. 6a-c
656 and Table 6) as both the root distribution profiles (Figs. 6a-c) and coefficients of
657 determination (Table 6) pointed out. It must be borne in mind, however, that a better
658 goodness of fit was obtained when data from the *in situ* meteorological station were
659 employed as inputs. This outcome, despite stressing the realistic behavior of RPDM,
660 also highlights the relevance of using relevant site-specific data for predicting root
661 distribution profiles accurately, given that a level of natural variability should be
662 expected even within one relatively small study site. In this sense, the RPDM root
663 profile predictions were larger when inputs from the other 6 meteorological stations
664 were considered (Figs. 6a-c), as the rainfall values (Table 4) and the chances for
665 deeper water infiltration in the soil were higher. Nonetheless, RPDM also envisaged

666 that when root systems were deeper, as a consequence of wetter conditions, the rooted
667 area in the uppermost soil horizons (i.e. 0-50 mm) would also be smaller compared to
668 our study site's drier conditions. This observation, although maybe related to resource
669 allocation issues (e.g. Schenk, 2005) captured by RPDM, was generated by the fact
670 that the plant biomass was not allowed to change under this wetter conditions and,
671 thus, it had to be distributed over a greater soil depth.
672 On the other hand, the root spread predictions for the plant species with the highest
673 biomass (i.e. *Rumex obtusifolius*) showed deeper and denser root systems, as
674 indicated before. The plant biomass determined the root system biomass (i.e. M_r; see
675 2.2.3) through the established plant-species-specific allometric relationship (see
676 4.3.2), in turn affecting the value of the scaling parameter (Ar_o; see 2.3.1) which
677 determined the root distribution profile. Thus, it can be expected that RPDM will
678 predict deeper and denser root systems for higher biomass and woody vegetation (e.g.
679 Gonzalez-Ollauri and Mickovski, 2014; see 4.4.2), as it is the case in reality
680 (Ekanayake and Phillips, 2002; Schenk and Jackson, 2002; Mickovski et al., 2008).
681 Nonetheless, it must be borne in mind that while for *Erigeron acris* and *Rumex*
682 *obtusifolius* the mean M_a between all the sampled individuals was utilized as input,
683 for *Silene dioica* a better output was obtained when using the sum of M_a for all the
684 studied individuals (RPDM C and D; Table 6). This outcome may be due to the
685 limited sample size and further research is recommended to clarify what approach
686 performs best for low biomass plant species.
687 With regard to the prediction of Ar_o and b (Table 6), RPDM projected values for both
688 parameters satisfactorily when the study site´s meteorological inputs were employed.
689 However, it must be borne in mind that he predicted b values were well below respect
690 to the values reported in Preti et al. (2010) for bushy species in a Mediterranean

691 setting. This outcome was expected given the climatic differences with our study site,
692 where AWC to plants is expected to accumulate at the soil surface, hence, leading to
693 shallower root systems in temperate humid climates as indicated in 4.3.1. Nontheless,
694 RPDM presented two main limitations in relation to the parameters Ar_o and b. On the
695 one hand, Ar_o is determined by the plant biomass and allometry. Since the latter
696 seemed not to be 'universal' in spite of the 'global' relationships for different plant
697 types and biomes reported in the literature (e.g. Cheng & Niklas, 2007), costly
698 species-specific information is needed to feed the model. On the other, b is entirely
699 dependent on the site's pedoclimatic conditions, meaning that the same mean rooting
700 depth is predicted regardless of the vegetation type, family or species.
701
702 4.4.2 Model sensitivity
703
704 The sensitivity analysis showed that RDPM is relatively sensitive (i.e. PV>20%) to
705 plant features (i.e. biomass and allometry) and to rainfall intensity, and relatively
706 insensitive (i.e. PV<20%) to the soil properties (Figs. 7a-d). The parameters that
707 presented a negative sensitivity index (SI) generated an opposite effect on the root
708 spread when they were higher in value. Contrariwise, those parameters that presented
709 a positive SI favored the development of bigger root systems when their value was
710 higher.
711 The two most sensitive, M_a and β, directly affect the proportion of root biomass (M_r),
712 the value of Ar_o for a given plant species, and the root system depth. A three fold
713 increase of ß , for instance, led to a drastic reduction of the root profile distribution
714 (Fig. 7c), whereas a three fold increase in plant biomass led to a considerably deeper
715 and wider root system profile (Fig. 7c). Again, these outcomes highlight how

716 important is to have species-specific information to accurately predict the distribution
717 of the root profile which would be easily obtained for known plant allometric
718 parameters. Regarding the third most sensitive parameter, as it has been discussed
719 previously, an increase of α would enhance the chances of deeper water infiltration in
720 the soil profile, favoring the development of root systems that explore the soil profile
721 deeper as deeper water will be available. In addition, the root mass density (ρ_r) was
722 relatively sensitive which highlighted the fact that plant-species specific values of ρ_r
723 easily estimated by the water volume displacement method (e.g. Hughes, 2005) could
724 lead to better root spread predictions.
725 The soil properties, even though shown to be insensitive, produced a subtle effect on
726 the root density distribution (i.e. $r(z)= b^{-1}e^{-z/b}$; Laio et al., 2006) that was captured by
727 RPDM (Fig. 7d) which may be related to the allocation and availability of resources
728 in the soil profile (Schenk, 2005). For example, a 10-fold decrease in organic matter
729 content led to a shallower and less extensive root system. On the contrary, a 3-fold
730 decrease in soil porosity led to a smaller but deeper root system that would be better
731 adapted to exploring and using resources deeper in the soil profile as observed in the
732 nature by the authors. As the plants can grow on nearly any substrate, and based on
733 our results, as well as the literature (e.g. Schenk and Jackson, 2002; Laio et al., 2006),
734 the plant root development would be mainly determined by the climate with the soil
735 properties affecting plant nourishment and wellbeing.
736
737 4.5 Spatially distributed RPDM
738
739 Spatially distributed RPDM successfully predicted a range of rooting depths (i.e.
740 $z_{95}=3b$) depending on the terrain features (Fig. 8). In this regard, RPDM predicted

shallower rooting depths for steeper terrain (i.e. lighter areas in Fig. 8) opposed to flat zones (i.e. darker areas in Fig. 8). The obtained outcome was consistent with the observations indicated in Hales et al. (2009), stating that vertical root distributions vary as a function of landscape position, likely encouraged by resources availability (Schenk, 2005). In this sense, topographical gradients may make water and nutrients less prone to accumulate along the slope gradient, being a plausible cause for shallower root spread in steep terrain. Additionally, plastic adaptations to which plants growing on slopes are subject to could also induce root spread alterations, such as the upslope root spread for plant anchorage purposes (Chiatante et al., 2003), which allegedly would prevent the root system from spreading downwards if the allometry holds. Nonetheless, it is worth noting that the model outcome was determined by the ability of RF to capture realistically the spatial heterogeneity of the soil properties driving root spread. In this sense, soil spatial input variables for RPDM (Table 3), obtained through implementing RF, showed a good fit with the environmental covariates in terms of the explained variance (Table 7). These outcomes therefore indicate that RF can be a powerful machine learning technique when applied to the prediction of soil spatial attributes. However, for the case of plant biomass, refinement of the employed covariates and inputs is needed to improve the model's output, as its goodness of fit was not that satisfactory. Additonally, other spatial covariates than the ones considered herein will have an influence on the spatial distribution of plant biomass (e.g. soil nutrients, sunlight exposure, etc.). We also believe that temporal data from more than just one growing season would enhance the model's quality as well, since the relationship, if any, between plant biomass and the other environmental covariates should be expected to be clearer with a larger dataset.

766 4.6. Mechanical effect of root spread on slope stability

767

768 When the root profiles from 4 random pixels were retrieved from within our study site
769 (Fig. 8; Points A, B, C and D), prediction differences in terms of root spread and soil-
770 root mechanical reinforcement were clearly observed (Figs. 9a-b). Vegetated flat
771 areas (e.g. Fig. 8, point B), for instance, presented considerably higher stability (Fig.
772 9b), as it could be expected. On sloping zones (i.e. Fig. 8, points A and D), however, a
773 denser plant cover (e.g. Fig. 8, point A) provided higher soil-root mechanical
774 reinforcement (Fig. 9a) and better stability conditions in depth (Fig. 9b). These
775 observations further verify the behavior of the spatially distributed RPDM.
776 In terms of the considered plant species under equal soil properties, the one with the
777 highest biomass (i.e. *Quercus robur*) presented the highest and deepest soil-root
778 mechanical reinforcement (Figs. 9c-d). Nonetheless, despite having assigned to the
779 former a T_r that doubled the one assigned to the herbaceous species (i.e. 8 MPa vs.
780 3.73 MPa), its mechanical reinforcement was comparable to the one provided by the
781 lowest M_a species (i.e. *Erigeron acris*). In fact, it was *Erigeron acris,* out of three
782 studied plant species, the one that showed the best performance from the soil
783 mechanical reinforcement point. This outcome has its origins in the values found for
784 the allometric fitting parameters (Table 6), which, as it has been stated, determine Ar_o
785 and ultimately scale the extent of the root spread. This issue led to *Silene dioica* to
786 present the lowest M_r and hence, the lowest mechanical effect (Figs 9c-d). In addition,
787 it supports the potential significance of plant allometry respect to root mechanical
788 reinforcement (Hwang et al., 2015), which should be further investigated as potential
789 cost-effective proxy for plant species selection in eco-engineering interventions, as
790 indicated before. Contrariwise, it is worth stressing the performance of *Rumex*

obtusifolius that, in turn, seemed to be also detected by its allometry. Despite having the highest biomass, and the deepest root spread (Fig. 7, Table 6), its mechanical reinforcement effect was considerably lower (χ^2=99, df=61) than for *Erigeron acris*, for which M_r was 4 times smaller on an individual basis (Table 6). However, when a fully-vegetated unit area of ground was considered, the belowground biomass for *Rumex* was nearly 6 times lower than for *E.acris* (i.e. 701.79 g vs. 4127.72 g) due to the found allometry and despite being the total aboveground biomass per unit area of ground (M_a^T) more than 4 times higher for *Rumex obtusifolius* (Table 6). Indeed, *Rumex obtusifolius'* root system is basically a taproot (Fig. 5) that, from the mechanical point, would mainly provide anchorage to the plant. Upon soil-slope failure this taproot would likely experiment a pullout mechanism (Mickovski et al., 2009) conferring less energy to the soil than root breakage (Waldron and Dakessian, 1981). Thus, its mechanical contribution to soil reinforcement should be assessed with a pullout model (e.g. Ennos, 1990) instead of with a breakage model and a root-added cohesion as it was the case here.

In any case, our model showed that all the considered plant species, besides *Silene dioica* (i.e. lowest M_r), would contribute noticeably to slope stability (Fig. 9d) within the topmost soil horizons. If predictions were confirmed, plant species like *Erigeron acris* could prevent the loss of up to 0.4 m^3 of soil per m^2 of land considering that there is a mechanical reinforcement of about 100 mm with respect to bare soil (Fig. 9d). However, no statistically significant differences were found between the 5 considered treatments (χ^2=7.82, df=4). This outcome may be due to not considering the hydrological effects of vegetation and assuming hydrostatic conditions in the soil profile. Under hydrodynamic conditions marked differences between bare and vegetated soil would be expected (Gonzalez-Ollauri and Mickovski, 2014). In this

816 sense, soil suction triggered by plant water uptake would enhance the soil stability
817 conditions (e.g. Wilkinson et al., 2002). In addition, it is worth noting that all the FoS
818 profiles converged in 1 (i.e. limit equilibrium) at the lower boundary of the soil
819 profile (Fig. 9d). This is produced due to setting 500 mm as the lower boundary of our
820 system (i.e. critical plane) and due to assuming cohesionless conditions to stress plant
821 effects.
822
823 5. Conclusions
824
825 Based on our observations and findings, it can be concluded that:
826
827 - Pioneer herbaceous plant species present shallow root systems in temperate
828 humid climates that can noticeably contribute to reduce soil loss and
829 landslides within the uppermost soil horizons.
830
831 - Root spread is largely determined by climatic conditions, precisely, by the
832 amount and distribution of rainfall, corroborating hydrotropism principles.
833
834 - Plant biomass and allometry are key to determine the degree of soil-root
835 reinforcement and, therefore, the eco-engineering potential of certain plant
836 species.
837
838 - Our model successfully predicts root spread in temperate humid climates on a
839 spatial basis, being its predictive capacity considerably improved when local
840 input data are employed.

- Machine-learning techniques, such as RF, present outstanding features to enhance the quality of spatial information and predictions.

- The hydrological effects of vegetation against landslides should be considered to have a better picture of the eco-engineering potential of given plant species. Furthermore, the relationship between plant allometry, climate and root-soil reinforcement, along with root tensile strength, should be further explored in light of an effective and sustainable selection of plant species. We also recommend testing our modelling approach on different plant species and communities and on different sites presenting similar climatic conditions for its final validation.

Acknowledgements

The authors thank the Catterline Brae Action Group (CBAG) for allowing us to carry this research on their brae, kindly supplying meteorological data and providing needed logistical and friendly support.

References

Alvarez-Uria, P. and Körner, C., 2007. Low temperature kimits of root growth in decidious and evergreen temperate tree species. Functional Ecology , 21, 211-218.

Allen, R., Pereira, L., Raes, D. and Smith, M., 1998. Crop evapotranspiration guidelines for computing crop water requirements. FAO Irrigation and drainage paper No 56.

BGS, 1999. British Geological Survey Rock Classification Scheme Vol. 3: Classification of sediments and sedimentary rocks. Research Report No RR 99-03. BGS, Nottingham, UK.

867 Bivand, R. S., Pebesma, E.J. and Gomez-Rubio, V., 2008. Applied Spatial Data Analysis with R.
868 Springer, New York, US.
869 Böhm, W., 1979. Methods of studying root systems; Ecological Studies 33. Springer-Verlag, New
870 York, US.
871 Breiman, L., 2001. Random Forests. Machine Learning , 45, 5-32.
872 BS 1377 Part 2, 1990. Methods of test for soils for civil engineering purposes. Classification tests.
873 British Standards Institution. London, UK.
874 Budyko, M., 1974. Climate and Life. Elsevier, New York, US.
875 Burylo, M., Hudek, C. and Rey, F., 2011. Soil reinforcement by the roots of six dominant species on
876 eroded mountainous marly slopes (Southern Alps, France). Catena , 84, 70-78.
877 Canadell, J., Jackson, R.B., Ehleringer, J.R., Mooney, H.A., Sala, O.E. and Schulze, E.D., 1996.
878 Maximum rooting depth of vegetation types at the global scale. Oecologia , 108, 583-595.
879 Casper, B., Schenk, H.J. and Jackson, R.B., 2003. Defining a plant's belowground zone of influence.
880 Ecology , 84 (9), 2313-2321.
881 Cheng, D. and Niklas, K.J., 2007. Above- and below-ground biomass relationships across 1534
882 forested communities. Annals of Botany , 99, 95-102.
883 Chiatante, D., Sarnataro, S., Di Iorio, A. and Scippa, G.S., 2003. The influence of steep slopes on root
884 system development. J. Plant Growth Regul. 21, 247-260.
885 Coelho, M.B., Villalobos, F.J. and Mateos, L., 2003. Modeling root growth and the soil-plant-
886 atmosphere continuum of cotton crops. Agricultrual Water Management, 60, 99-118.
887 Comino, E., Marengo, P. and Rolli, V., 2010. Root reinforcement effect of different grass species: A
888 comparison between experimental and models results. Soil & Tillage Research , 110, 60-68.
889 Cornelini, P., Federico, C., Pirrera, ., 2008. Arbusti autoctoni mediterranei per l'ingenieria
890 naturalistica. Primo contributo alla morfometria degli apparati radicali. Azienda Regionale Foreste
891 Demaniali Regione Siciliana-Collana, Sicilia n.40
892 Craig, R., 2004. Craig´s Soil Mechanics 7th Edition. E & FN Spon, London, UK.
893 Crow, P., 2005. The influence of soils and species on tree root depth. UK Forestry Commission ,
894 Edinburgh, UK.
895 Daniel, C., 1973. One-at-a-time-plans. Journal of the American Statistical Association , 68, 353-360.
896 Darwin, C., 1880. The power of movement in plants. John Murray, London, UK.

897 Deguchi, A., Hattori, S. and Park, H., 2006. The influence of seasonal changes in canopy structure on
898 interception loss: Application of the revised Gash model. Journal of Hydrology , 318, 80-102.
899 Doppler, T., Honti, M., Zihlmann, U., Weisskopf, P. and Stamm, C., 2014. Validating a spatially
900 distributed model with soil morphology data. Hydrol. Earth Syst. Sci., 18, 3481-3498.
901 Efron, B., 1979. Bootstrap methods: Another look at the Jackknife . Ann. Statist. , 1, 1-26.
902 Ekanayake, J.C. and Phillips, C.J., 2002. Slope stability thresholds for vegetated hillslopes: a
903 composite model. Canadian Geotechnical Journal , 39 (4), 849-862.
904 Ennos, A., 1990. The anchorage of leek seedlings: the effect of root length and soil strength. Annals of
905 Botany , 65, 409-416.
906 Enquist, B.J., Brown, J.H. and West, G.B., 1998. Allometric scaling pf plant energetics and population
907 density. Nature , 395, 163-165.
908 Félix, R., and Xanthoulis, D., 2005. Analyse de sensibilité du modèle mathématique “Erosion
909 Productivity Impact Calculator” (EPIC) par l’approche One-Factor-At-A- Time (OAT) .
910 Biotechnol. Agron. Soc. Environ. , 9 (3), 179-190.
911 GetMapping, 2014. GetMapping 2m resolution Digital Surface Model (DSM) for Scotland and Wales.
912 NERC Earth Observation Data Centre. Retrieved from
913 http://cataloque.ceda.uk/uuid/4b0ed418e30819e4448dc89a27dc8388
914 Gonzalez-Ollauri, A. and Mickovski, S.B., 2014. Integrated model for the hydro-mechanical effects of
915 vegetation against shallow landslides. EQA , 13, 35-59.
916 Hughes, S., 2005. Archimedes revisited: a faster, better, cheaper method of accurately measuring the
917 volume of small objects. Physics Education , 40 (5), 468-474.
918 Hales, T.C., Ford, C.R., Hwang, T., Vose, J.M. and Band, L.E., 2009. Topographic and ecologic
919 controls on root reinforcement. Journal of Geophysical Research , 114 (F03013), 1-17.
920 Head, K. H., 1980. Manual of Soil Laboratory Testing. CRC Press, Boca Raton, US.
921 Head, K. H., and Epps, R. J., 2011. Manual of Soil Laboratory Testing: Permeability. Shear Strenght
922 and Compressibility Tests (Vol. 2). CRC Press, Boca Raton, US.
923 Hijmans, R., 2014. Raster: Geographical data analysis and modeling. R package version 2.3-12 . URL:
924 http://CRAN.R-project.org/package=raster

925 Hwang, T., Band, L.E., Hales, T.C., Miniat, C.F., Vose, J.M., Bolstad, P.V., Miles, B. and Price, K.,
926 2015. Simulating vegetation controls on hurricane-induced shallow landslides with a distributed
927 ecohydrological model. Journal of Geophysical Research: Biogeosciences.
928 IPCC, 2014: Climate Change 2014: Synthesis Report. Contribution of Working Groups I, II and III to
929 the Fifth Assessment Report of the Intergovernmental Panel on Climate Change [Core Writing Team,
930 R.K. Pachauri and L.A. Meyer (eds.)]. IPCC, Geneva, Switzerland.
931 Jackson, R.B., Canadell, J., Ehleringer, J.R., Mooney, H.A., Sala, O.E. and Schulze, E.D., 1996. A
932 global analysis of root distributions for terrestial biomes. Oecologia , 108, 389-411.
933 Jenny, H., 1941. Factors of soil formation: A system of quantitative pedology. McGraw-Hill, New
934 York, US.
935 Kincardineshire Observer, 2013/4/11. Retrieved on 7/7/2015 from
936 http://www.kincardineshireobserver.co.uk/news/catterline-villagers-pull-together-to-clear-road-1-
937 2890185
938 Köppen, W., 1884. The thermal zones of the Earth according to the duration of hot, moderate and cold
939 periods and the impact of heat on the organic world. Meteorol. Z. , 1, 215-226.
940 Laan, P., Berrevoets, M.J., Lythe, S., Armstrong, W. and Blom, C.W.P.M., 1989. Root morphology
941 and aerenchyma formation as indicators of the flood-tolerance of rumex species. Journal of Ecology
942 , 77, 693-703.
943 Laio, F., D'Odorico, P., and Ridolfi, L., 2006. An analystical model to relate the vertical root
944 distribution to climate and soil properties. Geophysical Research Letters , 33, L18401.
945 Li, H., Han, X. and Wu, J., 2005. Lack of evidence for 3/4 scaling of metabolism in terrestial plants.
946 Journal of Integrative Plant Biology , 47 (10), 1173-1183.
947 Liaw, A. and Wiener, M., 2002. Classification and regression by randomForest. R News , 2 (3), 18-22.
948 Liess, M., Glaser, B. and Huwe, B., 2012. Uncertainty in the spatial prediction of soil texture:
949 comparison of regression tree and random forest models. Geoderma, 170, 70-79.
950 Lu, N. and Godt, J., 2008. Infinite slope stability under steady unsaturated seepage conditions. Water
951 Resources Research , 44 (W11404).
952 Lu, N. and Godt, J., 2013. Hillslope Hydrology and Stability. Cambridge University Press, New York,
953 US.

954 Malone, B., 2013. Use R for Digital Soil Mapping. Soil Security Laboratory, The University of Sidney,
955 Australia.
956 McMaster, G.S. and Wilhelm, W.W., 1997. Growing degree-days: one equation, two interpretations.
957 Agricultural and Forest Meteorology , 87, 291-300.
958 Mein, R.G. and Larson, C.L., 1973. Modeling infiltration during steady rain. Water Resources
959 Research , 9 (2), 384-394.
960 Mickovski, S., Hallet, P., Bransby, M., Davis, M., Sonnenberg, R., and Bengough, A., 2009.
961 Mechanical Reinforcement of Soil by Willow Roots: Impacts of Roots Properties and Root Failure
962 Mechanisms. Soil Sci. Soc. Am. , 73 (4), 1276-1285.
963 Mickovski, S., Hallett, P., Bengough, A., Bransby, M., Davies, M., and Sonnenberg, R., 2008. The
964 effect of willow roots on the shear strenght of soil. Advances in Geoecology , 39.
965 Neitsch, S., Arnold, J., Kiniry, J., and Williams, J., 2011. Soil and Water Assessment Tool; Theoretical
966 Documentation. Water Resources Institute Technical Report No 406. Texas, US.
967 Nicoll, B. and Amstrong, A., 1998. Development of Prunus root systems in a citystreet: pavement
968 damage and root architecture. The International Journal of Urban Forestry , 22 (3), 259-270.
969 Norris, J., Stokes, A., Mickovski, S., Cameraat, E., Van Beek, R., Nicoll, B., Achim, A., 2008. Slope
970 Stability and Erosion Control: Ecotechnological Solutions. Springer, Doerdrecht, The Netherlands.
971 Nunes, L., Lopes, D., Castro, F. and Gower, S.T., 2013. Aboveground biomass and net primary
972 production of pine, oak and mixed pine-oak forests on the Vila real district, Portugal. Forest
973 Ecology and Management , 305, 38-47.
974 O'Brien E.E., Brown, J.S. and Moll. J.D., 2007. Roots in space: a spatially splicit model for below-
975 ground competition in plants. Proc. R. Soc. B., 274, 929-934.
976 Odum, E. P. and Barrett, G.W., 1971. Fundamentals of Ecology. Thomson, Philadelphia, US.
977 Parzen, E., 1962. On estimation of probability density function and mode. The Annals of Mathematical
978 Statistics, 33, 1065-1076.
979 Perring, F.H. and Walters, S.M., 1982. Atlas of the British Flora. Botanical Society of the British Isles,
980 Cambridge, UK.
981 Prasad, A.M., Iverson, L.R. and Liaw, A., 2006. Newer classification and regression tree techniques:
982 bagging and random forest for ecological prediction. Ecosystems, 9, 181-199.

983 Preti, F., Dani, A., and Laio, F., 2010. Root profile assessment by means of hydrological, pedological
984 and aboveground vegetation information for bio-engineering purposes. Ecological Engineering , 36,
985 305-316.
986 Priestley, C., and Taylor, R., 1972. On the Assessment of Surface Heat Flux and Evaporation Using
987 Large-Scale Parameters. Monthly Weather Review , 100 (2), 81-92.
988 R Development Core Team, 2014. R: A language and environment for statistical computing. Viena,
989 Austria: R Foundation for Statistical Computing URL: http://www.R-project.org
990 Reynolds, W. D. and Elrick, D. E., 1990. Ponded Infiltration From a Single Ring: I, Analysis of Steady
991 Flow. Soil Sci. Soc. Am. J. , 54, 1233-1241.
992 Savabi, M.R., Engman, E.T., Kustas, W.P., Rawls, W.J. and Kenemasu, E.T., 1989. Water balance and
993 percolation. In L. a. Lane, USDA-Water Erosion Prediction Project: Hillslope Profile Model
994 Documentation (Vol. Chapter 7). West Lafayette, US: USDA-ARS National Soil Erosion Research
995 Laboratory.
996 Scharmer, K. and Greif, J., 2000. The European solar radiation atlas, Vol 2: Database and exploitation
997 software. Les Presses de l'Ecole de Mines, Paris, France.
998 Schenk, H., 2005. Vertical vegetation structure below ground: scaling from root to globe. Progress in
999 Botany , 66, 341-373.
1000 Schenk, H.J. and Jackson, R.B., 2005. Mapping the global distribution of deep roots in relation to
1001 climate and soil characteristics. Geoderma , 126, 129-140.
1002 Schenk, H., and Jackson, R., 2002. The global biogeography of roots. Ecological Monographs , 72 (3),
1003 311-328.
1004 Schulte, E. and Hopkins, B.G., 1996. Estimation of soil organic matter by weight loss-on-ignition. In
1005 Magdoff, F. et al. *Soil Organic Matter: Analysis and Interpretation* (pp. 21-31). Soil Sci. Soc. Am.,
1006 Madison, US.
1007 Stokes, A., Douglas, G., Fourcaud, T., Giadrossich, F., Gillies, C., Hubble, T., et al., 2014. Ecological
1008 mitigation of hillslope instability: ten key issues facing researchers and practitioners. Plant Soil ,
1009 377, 1-23.
1010 Stokes, A., Norris, J., van Beek, L., Bogaard, T., Cammeraat, E., Mickovski, S., et al., 2008. How
1011 vegetation reinforces soil on slopes. In J. Norris, A. Stokes, S. Mickovski, E. Cammeraat, R. van

1012 Beek, B. Nicoll, et al., Slope Stability and Erosion Control: Ecotechnological Solutions (pp. 65-
1013 116). Springer, Dordrecht, The Netherlands.
1014 Tardio, G. and Mickovski, S. B., 2016. Implementation of eco-engineering design into existing slope
1015 stability design practices. *Ecological Engineering*, 92: 138-147
1016 Toth, B., Weynants, M., Nemes, A., Mako, A., Bilas, G. and Toth, G., 2015. New generation of
1017 hydraulic pedotransfer functions for Europe. European Journal of Soil Science , 66, 226-238.
1018 Tsutsumi, D., Kosugi, K. and Mizuyama, T., 2003. Effect of Hydrotropism on Root System
1019 Development in Soybean (Glycine max): Growth Experiments and Model Simulation. J. Plant
1020 Growth Regul. , 21, 441-458.
1021 Tron, S., Dani, A., Laio, F., Preti, F. and Ridolfi, L., 2014. Mean root depth estimation at landslide
1022 slopes. Ecological Engineering , 69, 118-125.
1023 UK Met Office. MIDAS Land Surface Stations data, 1853-current. Retrieved from
1024 http://badc.nerc.ac.uk/view/badc.nerc.ac.uk_ATOM_dataent_ukmo-midas
1025 UNEP (United Nations Environmental Programme),1992. World atlas of desertification . UNEP,
1026 London, UK.
1027 Urbano, P., 1995. Tratado de fitotecnia general. Mundi-Prensa, Madrid, Spain.
1028 USDA-NRCS, 1997. National grazing lands handbook. USDA-NRCS, Washington DC, US.
1029 van Beek, R., Cammeraat, E., Andreu, V., Mickovski, S., & Dorren, L., 2008. Hillslope processes:
1030 mass wasting, slope stability and erosion. In J. e. Norris, Slope stability and erosion control:
1031 Ecotechnological solutions (pp. 17-64). Springer, Dordrecht, The Netherlands.
1032
1033 vor de Poorte, P., 2011. Retrieved 7/24/2015 from PEDROX: live weather from Catterline:
1034 http://www.pedrox.com
1035 Waldron, L.J. and Dakessian, S., 1981. Soil reinforcement by roots: calculation of increased soil shear
1036 resistance from root properties. Soil Science , 132 (6), 427-435.
1037 Waldron, L. J., 1977. The Shear Resistance of Root-Permeated Homogeneous and Stratified Soil. Soil
1038 Sci. Soc. Am. J , 41 (5), 843-849.
1039 West, G.B., Brown, J.H. and Enquist, B.J., 1997. A general model for the origin of allometric scaling
1040 laws in biology. Science , 276, 122-126.

1041 Wilcox, R.R. and Keselman, H.J., 2003. Modern robust data analysis methods: Measures of central
1042 tendency. Psychological Methods , 8 (3), 254-274.
1043 Wilkinson, P.L., Anderson, M.G. and Lloyd, D.M., 2002. An integrated hydrological model for rain-
1044 induced landslide prediction. Earth Surface Processes and Landforms , 27, 1285-1297.
1045 Wu, H., McKinnell, W. and Swanston, D., 1979. Strength of tree roots and landslides on Prince of
1046 Wales Island, Alaska. Canadian Geotechnical Journal , 16 (1), 19-33.
1047 Wu, L., McGechan, M.B., Watson, C.A. and Baddeley, J.A., 2005. Developing existing plant root
1048 system architecture models to meet future agricultural challenges. Advances in Agronomy , 85,
1049 181-219.
1050 Yang, Y., Fang, J., Ji, C. and Han, W., 2009. Above- and belowground biomass allocation in Tibetan
1051 grasslands. Journal of Vegetation Science , 20, 177-184
1052
1053